Interferometric Measurements of Bridges Displacements and Scattering Mechanisms

Liudmila Zakharova, FIRE RAS, Vvedensky sq., 1, Fryazino 141190, Russia
tel. +7 49656 52432, fax +7 49656 52407 e-mail: ludmila@sunclass.ire.rssi.ru
Alexander Zakharov, FIRE RAS, aizakhar@sunclass.ire.rssi.ru, Russia

Abstract

The paper aims at bridges displacement evaluation. Sentinel-1 high resolution SAR data provides with detailed images of selected bridges. Two types of bridge design were selected: suspension bridges as rather flexible objects, and a girder bridge with its stiffness as a more stationary target. Vertical displacements of suspension bridges reach up to 12,6 cm for 12-days time interval. A girder bridge crossing a quiet river shows small shifts between its parts in the phase image of its upper surface, and in addition in the phase image of its underneath due to triple-bounce scattering mechanism and almost windless weather. Vertical displacements of 9 mm were registered.

1 Introduction

SAR interferometry is a useful tool for measuring surface displacements of different nature: seismic shifts [1], slow sea-coast subsidence [2], glacier motion [3], frost mounds [4] etc. High-resolution SARs of new generation allow estimating displacements of man-made constructions, and, in particular, bridges [5]. In this study we focus at two types of bridges: suspension bridges over sea straits and girder bridges over quiet lowland rivers. Suspension bridges were expected to be non-stationary, and our goal was to estimate the rate of their displacement. Girder bridges are more stiffened by their design, so expected displacements should be smaller than for suspension bridges. Finally, for the first time we estimate phase difference on the multiple-bounce image of a bridge, and it is in accordance with measurements on the main single-bounce backscatter mechanism.

2 Suspension Bridges Displacements

A suspension bridge's deck has relatively low stiffness due to design of this type of bridges, therefore it can shift between SAR observations because of live loads and dynamic loads (e.g., wind). The displacement can be measured by means of SAR interferometry.

In our study we use two pairs for San Francisco area, and one pair for Istanbul, Turkey. Both scenes include sea straits and bays and a number of bridges.

The famous Golden Gate bridge shows good coherence in the pair with dates of observation September 8 and 20, 2016: the mean coherence value along the bridge image is 0.41, standard deviation is equal to 0.17. Phase profile is in the **Figure 1**. There are several 2π-jumps in the plot due to wrapped phase. After unwrapping procedure one can obtain a plot with a two-bulge top between pixels 70-75 and very steep slopes. Unwrapped phase variation runs to 9π. This may imply a displacement of 12.6 cm in the line-of-sight direction. In fact, this value is not reliable because of very fast phase increasing/decreasing along the bridge. Some of phase jumps can be wrong interpreted on the phase unwrapping step and cause a 2.8-cm error in the displacement measurements.

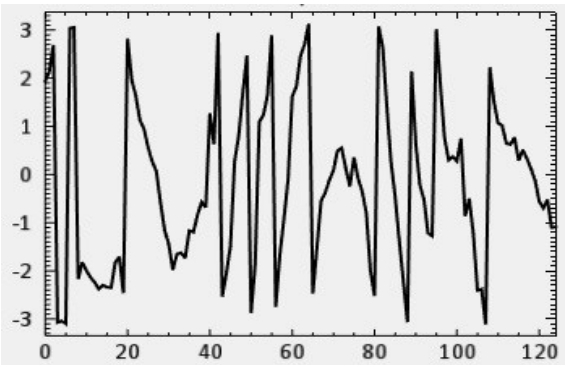

Figure 1: Phase profile along the Golden Gate bridge. X: pixels. Y: interferometric phase in radians.

The same scene includes another suspension bridge that connected San Francisco to Yerba Buena Island, it is a western part of San Francisco-Oakland Bay Bridge. This part is a double suspension bridge: there is a concrete anchorage in the middle of the bay and two suspension spans on each side of it. Coherence image of the whole western part demonstrates high values: the mean is equal to 0.42 with standard deviation 0.19. After phase unwrapping procedure the phase profile looks like two hollows of 5.5π depth, the centers of the hollows correspond to the central parts of each bridge. The direction of the displacement is opposite to the previous case: the Golden Gate bridge's center uplifted with respect to its ends in between the observations, and the Oakland suspension

ISBN 978-3-8007-4636-1 / ISSN 2197-4403

bridges' centers subsided during the same 12-days interval. The rate of the shift is maximal near the centers of the bridges, where it runs to 8.2 cm.

The last suspension bridge in this study is Third Bosphorus Bridge. It is located near the Black Sea entrance of the Bosphorus strait in Turkey. The bridge's design is a combination of cable-stayed and suspension types in order to ensure the bridge's deck stability for safe railway traffic. Coherence values along the bridge are good, the mean is 0.56 with standard deviation equal to 0.17. Phase profile is in the **Figure 2**.

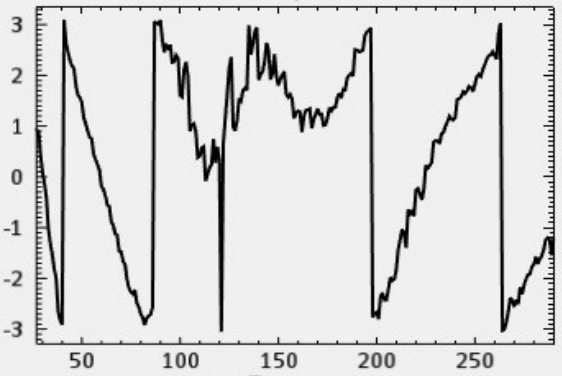

Figure 2: Phase profile along the Third Bosphorus bridge. X: pixels. Y: interferometric phase in radians.

In the Figure 2 we can see four explicit phase jumps, and unwrapped procedure phase profile has about 4π in depth. This value corresponds to 5.1 cm of vertical uplifting of the bridge's center between the observations. The central part with additional vertical suspenders corresponds approximately to pixels 70-230. Slant cables from the left and right bridge's pylons reach pixels 0-114 and 186-300, thus a part of the bridge between pixels 100 and 180 is suspended-only and has no additional support. In the interferogram there are two details that have relation to the suspended-only part of the bridge: firstly, phase noise level is higher in the neighbourhood of this part and, secondly, there is a local maximum of the plot at the bottom of the 4π-depth pit, the center of this positive deviation of the phase is near the pixel 140. Thus one can state that the central suspended part of the bridge is less stable with respect to cable-stayed parts, and that there is a small-scale displacement component in the direction that is opposite to the whole displacement picture. Generally, the Third Bosphorus bridge demonstrates the smallest displacement rate (5 cm/12 days) and the highest coherence (0.56), that confirms the stiffness of the combined cable-stayed and suspension design. In the **Table 1** displacement rates for three bridges are summarized.

Bridge	Length, m	Vertical displacement, cm
Golden Gate	1970	-12.6
Oakland-SF, west span	1470	8.2
Third Bosphorus Bridge	2100	5.1

Table 1: Measurement of displacements of three suspension bridges.

In the end of this section it is worth noting that the second interferometric pair for the area of San Francisco shows low coherence of the Golden Gate bridge (0.25), while the Oakland bridge's coherence becomes even better (0.47), and it demonstrates the same displacement rate of about 8 cm for the 12-days interval. Difference between the pairs is in the orbit direction (ascending/descending). The Golden Gate bridge's orientation in the interferogram with low coherence is near-azimuthal (slant range of all pixels is about the same). Such observation geometry with 13.9 meters of Sentinel-1 azimuth resolution results in very fast phase change along the bridge and, consequently, low coherence. As for the Oakland bridge, it's orientation is near-range in both interferograms, thus the measurements are possible and give near the same value of displacement about 9 cm.

Two Turkish suspension bridges are the additional illustration to the different resolution in slant range and azimuth: the Osman Gazi bridge that crosses the Izmit bay constitutes 18° with the flight direction, and the coherence in it is extremely low (it was not discussed above because of lack of phase information); whereas the Third Bosphorus bridge within the same frame is oriented perpendicularly to the flight direction, and the coherence along it is significantly higher.

3 Phase measurements in the triple-bounce image of a bridge

In the previous sections we didn't take into account the multiple "ghost" images of the bridges, because in the interferometric context a reflection from the water surface is followed typically by the total loss of coherence and uselessness of phase measurements. It is the case for strait bridges with a wavy water surface underneath. But bridges over slow lowland rivers can show good coherence in the triple-bounce under proper weather conditions.

The Striginsky bridge over Oka River near Nizhniy Novgorod, Russia, is a girder concrete bridge with five abutments within the riverbed and two additional abutments, by one for each river bank. Total length of this highway bridge is about 950 m. Fragment of the amplitude image, coherence image and interferogram containing the bridge are in the **Figure 3**. In the amplitude image one can see

three near-vertical bright dashed threads of the main image of the bridge. These threads indicate borders of the bridge and central traffic divisor's metallic constructions. The roadbed between is smooth enough, and the backscatter from it is extremely low. The fourth brighter line is almost solid: it is a "ghost" image of the bridge, which is a result of double-bounce signal scattering from a water surface and the bridge's side. And, finally, a thick very bright strip to the right of it is a three-bounce image of the bottom side of the bridge with the first and the third bounce reflected from the water, and the second one from the bridge's underneath. One can find these three types of images in majority of high-resolution SAR images of bridges (e.g., in [6]).

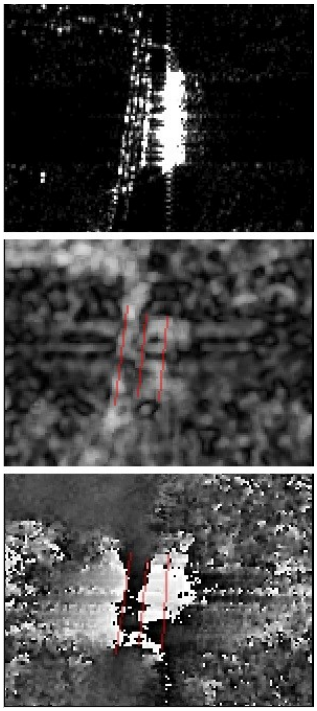

Figure 3: Striginsky bridge: amplitude image (top), coherence image (center), and phase image (bottom). Red lines mark profiles location in the coherence and phase images.

Suspension bridges from the section 2 demonstrate multiple images, too, and some of them show even more than three images. All of these sea bridges have wavy water surface under them, therefore all double-, three- and more-bounce images have very low coherence. River water can be smooth under suitable weather conditions, e.g., low wind speed. For the pair April 18-30, 2017, web-archive reports low wind (2-3 m/sec on both dates), so we can expect mirror reflection from water.

In the middle of the Figure 3 there is a coherence image for Striginsky bridge, and we can see bright areas of higher coherence not only for the main bridge image, but also for multiple-bounce images. Mean value of interferometric coherence is equal to 0.47 for single-bounce bridge image, 0.3 for the double-bounce, and 0.46 for the triple-bounce. As a double-bounce scattering mechanism always projects signal returns from the bridge's side illuminated by SAR onto a narrow line in the image, it's coherence is low because of effect which is similar to foreshortening. We can expect a clear phase image with a good coherence only if the bridge's side has a vertical size which is comparable to SAR's range pixel spacing.

Phase profiles for odd-bounce images of the Striginsky bridge is in the **Figure 4**. In the single-bounce profile one can see that phase is not fast-changing, it's total variation is 1.5 radians, that corresponds to 9 mm of the vertical shift. Thus, the surface of the bridge is rather stabilized, with possible shift rate under 1 cm. The shift is clear seen between the first and the second abutments which are located in the pixel 1 and 8, respectively. The third abutment is located in the center of the river (pixel 17). It's phase value is close to the first abutment's phase. The fourth one at the pixel 23 gives a low phase value under zero again, and the fifth abutment (pixel 31) has a close phase value. In general, we can state two local minima at abutments 2 and 4 that correspond to slight uplift with respect to other three abutments.

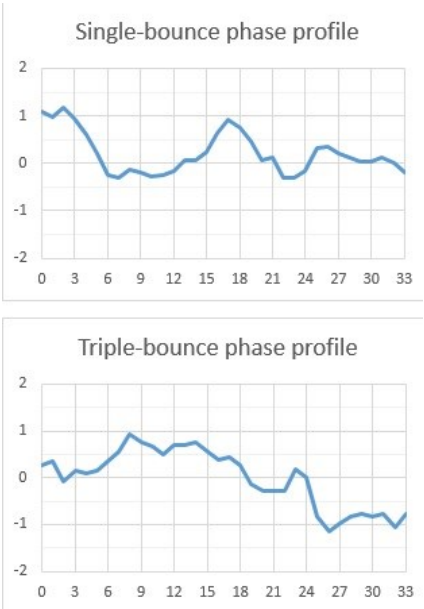

Figure 4: Phase profiles for single- and triple-bounce bridge images. X: pixels. Y: phase in radians. Pair April 18-30, 2017.

The bottom plot in the Figure 4 shows the phase values of the triple-bounce image of the bridge. Around pixels 8 and 23 there are two local maxima. It means that we see the same displacement of the bridge: if a part of the bridge slightly uplifts, its top becomes closer to the SAR,

ISBN 978-3-8007-4636-1 / ISSN 2197-4403

and its underneath becomes farther from the water surface, and signal path length increases. Thus, the inverse form of the second plot confirms the mutual shifts of the bridge's fragments.

The pair of fall observations September 14-26, 2016, shows more clearly two minima around the 2nd and the 4th abutments and a maximum in between. One can see also an inverse form of the triple-bounce plot for this pair in the **Figure 5**. Unfortunately, lack of good coherence in other pairs (acquired in winter-spring 2016-2017) prevents from an inference about nature of these displacements.

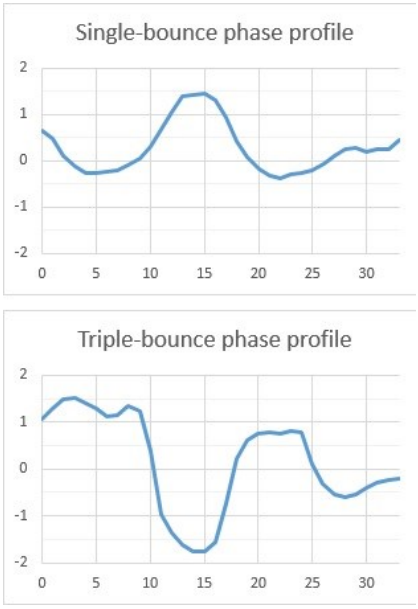

Figure 5: Phase profiles for single- and triple-bounce bridge images. X: pixels. Y: phase in radians. Pair September 14-26, 2016.

Most of processed summer pairs show low coherence of the double- and triple-bounced image of the bridge, so we cannot implement analysis of multiple images described above. Only two summer 12-days interferograms keep coherence relatively high for a triple-bounce image. Phase profiles for the pair August 16 – August 28, 2017, are in the **Figure 6**. We can see once more inversion of the curve form (Pearson correlation coefficient for two profiles is –0.75), but the single-bounce profiles has more small-scaled features (e.g., between pixels 15 and 20). Absence of them in the 3-bounce phase image designates that these phase behavior can be related to the changes on the surface of the bridge only: it can be displacement of some fragment of the bridge's border. One of the plots' fragment in the **Figure 6** shows similar behavior of the single- and triple-bounce: phase decreases in both plots between pixels 3 and 9. It can be related to horizontal displacement of the bridge fragment: in the opposite to vertical displacement, horizontal one should produce two consisted phase plots for single- and triple-bounce images. Phase difference between pixels 3 and 9 is equal to 0.7 rad and 0.2 rad, for 1- and 3-bounce, correspondingly. This means horizontal displacement under 1 cm. Influence of the horizontal component of a total displacement can explain the difference in the phase variances in the Figure 5 between pixels 10 and 20: it constitutes 1.5 rad for the single-bounce profile, and 2.2 rad for the triple-bounce. In the case of vertical-only motion a total variations should be close to each other, but the presence of additional horizontal component results exactly in this way: it changes the value of total variation for a single- and a triple-bounce phase in the opposite directions.

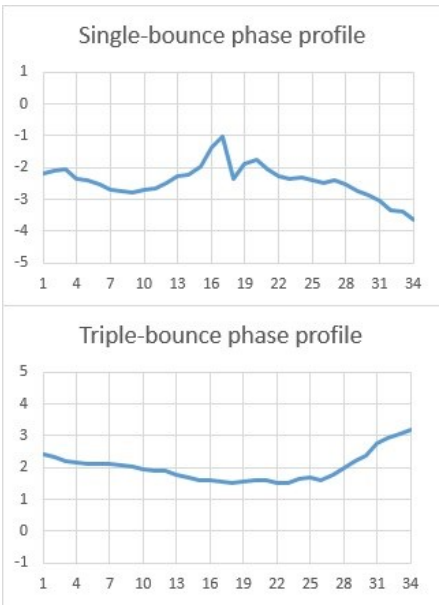

Figure 6: Phase profiles for single- and triple-bounce bridge images. X: pixels. Y: phase in radians. Pair August 16-28, 2017.

4 Conclusions

Two types of bridges were investigated by means of SAR interferometry: suspension bridges and girder bridge.

Suspension bridges demonstrated vertical displacements in the scale of first centimeters for a 12-days interval: 5 cm for the Third Bosphorus bridge, 8 cm for the west span of San Francisco - Oakland bridge, and 12 cm for the Golden Gate bridge. Different signs of bridges' motion direction indicate that the registered displacements compensate each other on longer intervals, and the cause

ISBN 978-3-8007-4636-1 / ISSN 2197-4403

of detected bridges' "breath" is dynamic load. Better resolution in azimuth will help to examine suspension bridges which direction coincides with flight direction.

Girder bridge's displacement over lowland rivers can be estimated from both sides of a bridge due to multiple-bounce mechanism. For Striginsky bridge we discovered small mutual shifts below 1 cm. Phase increase along the bridge here is slow with comparison to the interferogram of the Golden Gate bridge, thus azimuthal direction of the Striginsky bridge is not an obstacle in this case. Displacements were detected in autumn and spring interferograms. Low wind during the observations allows seeing shifts from underneath of the bridge, thus we can exclude the hypothesis of surface-only shifts. Further research can discover a type and cause of the bridge's motion.

References

[1] D. Massonnet et al.: *The displacement field of the Landers earthquake mapped by radar interferometry,* Nature, 1993, Vol. 364, No. 8, 138—142.

[2] T. Strozzi, L. Tosi, U. Wegmuller, C. Werner, P. Teatini, L. Carbognin: *Land subsidence monitoring service in the Lagoon of Venice*, Proceedings of IEEE International Geoscience and Remote Sensing Symposium (IGARSS), 21-25 July 2003, 212-214.

[3] P. Prats, R. Scheiber, A. Reigber, C. Andres, R. Horn: *Estimation of the Surface Velocity Field of the Aletsch Glacier Using Multibaseline Airborne SAR Interferometry,* IEEE Transactions on Geoscience and Remote Sensing, Vol. 47, Issue 2, Feb. 2009, 419 – 430.

[4] Chimitdorzhiev T.N., Dagurov P.N., Bykov M.E., Dmitriev A.V., Kirbizhekova I.I.: Comparison of ALOS PALSAR interferometry and field geodetic leveling for marshy soil thaw/freeze monitoring, case study from the Baikal lake region, Russia // Journal of Applied Remote Sensing. 2016. T. 10. № 1.

[5] Lazecky M., Perissin D., Bakon M., de Sousa J.M., Hlavacova I., Real N., Potential of satellite InSAR techniques for monitoring of bridge deformations, Proc. 2015 Joint Urban Remote Sensing Event (JURSE), Lausanne, Switzerland, 2015.

[6] J.-S. Lee, E. Krogager, T.L. Ainsworth, and W.-M. Boerner: *Polarimetric analysis of radar signature of a manmade structure*, IEEE Remote Sensing Letters, 3(4), 555–559, October 2006